

## Orientation Correlations in Lamellar Block Copolymers

B. A. Garetz,\* N. P. Balsara,\* H. J. Dai, Z. Wang, and M. C. Newstein

*Departments of Chemistry, Chemical Engineering, Materials Science, and Electrical Engineering, Polytechnic University, Six Metrotech Center, Brooklyn, New York 11201*

B. Majumdar

*Corporate Research Process Technologies Laboratory, 3M Company, Building 208-1-01, St. Paul, Minnesota 55144**Received January 16, 1996; Revised Manuscript Received April 11, 1996*

**ABSTRACT:** Orientation correlations in a quiescently quenched, lamellar block copolymer were examined by a combination of depolarized light scattering and transmission electron microscopy. These experiments reveal exponential correlation functions with characteristic lengths that depend on the thermal history of the sample. The correlation lengths obtained from light scattering and electron microscopy are in reasonable agreement.

## Introduction

Many materials of biological and commercial importance comprise stacks of microscopic layers: biological membranes, metallic alloys, and lamellar phases formed by surfactants and block copolymers. In the absence of external fields, these materials consist of locally ordered, but globally disordered stacks or grains, with concomitant point, line, and wall imperfections. Aspects of these assemblies are well understood due to several decades of theoretical and experimental effort.<sup>1–4</sup> The average layer spacing has been obtained by small-angle X-ray and neutron scattering. Optical microscopy and electron microscopy have been used to investigate the topology of imperfections. A feature of interest that has escaped quantitative analysis is the extent of local coherence of the lamellae. Finite coherence and imperfections are nonequilibrium features, determined not only by the state of the sample but also by its history. Material properties such as stress–strain relationships and permeability are dependent on these features. In this paper, the statistical properties of quiescently quenched block copolymer lamellae were obtained by a combination of transmission electron microscopy (TEM) and depolarized light scattering. These experiments reveal that an exponential function describes the correlation between lamellar orientations at different points in the material. In related studies concerning correlations in disordered and partially ordered media, Levitz et al. have examined density correlations in Vycor glass,<sup>5</sup> while Murray and co-workers have studied bond-orientation correlations in two-dimensional colloidal suspensions.<sup>6</sup>

## Experimental Section

A polystyrene–polyisoprene diblock copolymer was synthesized by anionic polymerization under high vacuum. The weight-averaged molecular weights of the polystyrene and polyisoprene blocks were determined to be 11 and 7 kg/mol, respectively, and we refer to this polymer as SI(11–7); polydispersity index of the polymer = 1.07. At low temperatures, this copolymer forms alternating polystyrene and polyisoprene lamellae. At high temperature, this copolymer exhibits a liquid-like disordered phase. The transition from order to disorder occurs at  $121 \pm 3$  °C.<sup>7</sup>

Depolarized light scattering and electron microscopy experiments were conducted on SI(11–7) melts, encased in 0.74 cm

diameter glass cuvettes. The same samples were used in both experiments. The samples were first heated to 130 °C to erase thermal history and then rapidly cooled to 115.5 °C. The samples were tempered at this temperature for variable lengths of time, and the depolarized light scattering profiles were monitored during this process. The instrument used for these measurements is described in ref 8. We present data from two samples, T50 and T900, which were tempered for 50 and 900 min, respectively. The scattering data were not converted to absolute scattering cross-sections. Time zero is defined as the time at which the temperature change was initiated, and it took about 15 min for the sample temperature to reach 115.5 °C. After tempering, both samples were cooled rapidly to room temperature. The polystyrene lamellae undergo a glass transition at 100 °C, thus preserving the structure formed at 115.5 °C. The samples were then removed from the cuvettes and stained with OsO<sub>4</sub>, and ultrathin (30 nm in thickness) sections were obtained using a Reichert Ultramicrotome at –120 °C. The sections were examined on a Jeol 1210 transmission electron microscope.

## Theory

A lamellar block copolymer sample which is created in the absence of external fields may be considered to be locally uniaxial with the optic axis perpendicular to the lamellar planes. The widths of the block copolymer lamellae are much smaller than  $\lambda$ , the wavelength of light, and are not directly probed by optical methods. The direction of the optic axis varies from point to point, and this results in depolarized ( $V_H$ ) light scattering.<sup>8–11</sup> The methodology for computing  $V_H$  scattering from such systems was pioneered by Stein and Wilson.<sup>9</sup> Let  $\{y, x\}$  refer to the polarization direction of the {scattered, incident} beam propagating in the  $z$ -direction. If the deviation of the  $yx$  element of the dielectric permittivity tensor at the point  $\mathbf{r}$ , from its average scalar value, is represented by  $\delta\epsilon_{yx}(\mathbf{r})$ , then the statistical quantity relevant to  $V_H$  scattering is the correlation function  $C(\mathbf{r}, \mathbf{r}')$ :

$$C(\mathbf{r}, \mathbf{r}') = \frac{\langle \delta\epsilon_{yx}(\mathbf{r}) \delta\epsilon_{yx}(\mathbf{r}') \rangle}{\langle \delta\epsilon_{yx}(\mathbf{r})^2 \rangle} \quad (1)$$

where  $\langle \dots \rangle$  represent ensemble averages.

The correlation function has a value of unity when  $\mathbf{r} = \mathbf{r}'$  and drops toward zero as  $|\mathbf{r} - \mathbf{r}'|$  becomes large. Taking the  $z$ -direction to be the polar axis for the spherical polar angles  $\theta(\mathbf{r})$  and  $\phi(\mathbf{r})$  giving the direction of the optic axis at point  $\mathbf{r}$ , we have

\* Authors to whom correspondence should be addressed.

\* Abstract published in *Advance ACS Abstracts*, May 15, 1996.

$$\frac{\delta\epsilon_{yx}(\mathbf{r})}{\epsilon_0} = n(n_e - n_o) \sin^2 \theta(\mathbf{r}) \sin[2\phi(\mathbf{r})] \quad (2)$$

where  $\epsilon_0$  is the average dielectric permittivity of the medium,  $n$  is the average refractive index of the medium, and  $n_e$  and  $n_o$  are the local extraordinary and ordinary refractive indices, respectively.

The  $y$ -polarized power per unit solid angle scattered in the direction of the unit vector  $\mathbf{s}$  from an  $x$ -polarized beam of intensity  $I_{\text{in}}$  W/m<sup>2</sup> is

$$I(q) = \frac{k^4 I_{\text{in}}}{(4\pi)^2} \int d\mathbf{r} \int d\mathbf{r}' C(\mathbf{r}, \mathbf{r}') \exp[-i\mathbf{q} \cdot (\mathbf{r} - \mathbf{r}')] \quad (3)$$

where the propagation constant  $k = 2\pi/\lambda$ ,  $\lambda$  is the wavelength of the incident beam, and the scattering vector,  $\mathbf{q}$ , is given by

$$\mathbf{q} = \frac{2\pi}{\lambda} (\mathbf{s} - \mathbf{e}_z) \quad (4)$$

$\mathbf{e}_z$  is the unit vector in the  $z$ -direction.

Equation 3 is only valid in the limit of single scattering. This is appropriate for the block copolymer samples studied here because they were highly transparent. This is expected, due to the weak optical anisotropy of the ordered regions;  $|n_e - n_o|$  is estimated to be  $10^{-4}$  (see ref 8).

For a globally isotropic sample, the correlation function depends on the vector difference  $(\mathbf{r} - \mathbf{r}')$ . If the correlation function depends only on the magnitude  $|\mathbf{r} - \mathbf{r}'|$ , then the  $V_H$  scattered intensity is axially symmetric and is given by

$$I(q) = \frac{k^4 I_{\text{in}} V n^2 (n_e - n_o)^2}{15\pi} \int_0^\infty r^2 C(r) \frac{\sin(qr)}{qr} dr \quad (5)$$

where  $V$  is the illuminated sample volume.

One can thus obtain  $C(r)$  in block copolymers by measuring the  $V_H$  light scattering profile and using eq 5. On the other hand, specific models, based on assumptions regarding the nature of the correlation function, allow us to cast eqs 1 and 2 into forms that can be used to obtain  $C(r)$  from TEM images. We present two models which provide independent methods for computing  $C(r)$ .

**Model 1:** If we take  $\theta(\mathbf{r})$  and  $\phi(\mathbf{r})$  to be statistically independent in their variation with position in the sample, then eqs 1 and 2 give

$$C(|\mathbf{r} - \mathbf{r}'|) = \left\{ \frac{15}{8} \langle \sin^2 \theta(\mathbf{r}) \sin^2 \theta(\mathbf{r}') \rangle \right\} \langle \cos[2\{\phi(\mathbf{r}) - \phi(\mathbf{r}')\}] \rangle \quad (6)$$

where we have used the fact that  $\langle \cos[2\{\phi(\mathbf{r}) + \phi(\mathbf{r}')\}] \rangle = 0$ .

The first term within curly brackets in eq 6 decays from 1 when  $|\mathbf{r} - \mathbf{r}'| \rightarrow 0$  down to  $5/6$  when  $|\mathbf{r} - \mathbf{r}'| \rightarrow \infty$ . Thus the decay of the correlation function is dominated by the last term in eq 6, which decays from 1 when  $|\mathbf{r} - \mathbf{r}'| \rightarrow 0$  down to 0 when  $|\mathbf{r} - \mathbf{r}'| \rightarrow \infty$ . To a good approximation (within 17%),

$$C(|\mathbf{r} - \mathbf{r}'|) \approx \langle \cos[2\{\phi(\mathbf{r}) - \phi(\mathbf{r}')\}] \rangle \quad (7)$$

Equation 6 is equivalent to that used by Stein and Wilson to analyze light scattering from semicrystalline polymers,<sup>9</sup> except for our assumption regarding the statistical independence of  $\theta(\mathbf{r})$  and  $\phi(\mathbf{r})$ . The assumption allowed us to approximate the correlation function in terms of the local polar angle,  $\phi$ , only. This was necessary in our case because, as illustrated in the

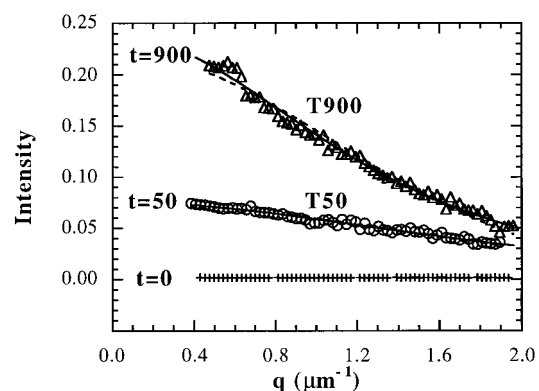


**Figure 1.** Depolarized light scattering intensity profiles (intensity versus scattering vector,  $q$ ) as a function of tempering time,  $t$ , in minutes. The curves represent least-squares fits through the data: solid curves, square Lorentzian fits; dashed curves, Gaussian fits. The two kinds of fits are indistinguishable for the T50 sample.

Results and Discussion section, only  $\phi(\mathbf{r})$  can be measured directly by TEM.

**Model 2:** If we assume that the sample consists of space-filling, "ideal grains" with (1) constant optic axis within a grain, (2) no correlation between grain shape and optic axis, and (3) no correlation between optic axes of different grains, then<sup>8</sup>

$$C(|\mathbf{r} - \mathbf{r}'|) = \text{probability that both } \mathbf{r} \text{ and } \mathbf{r}' \text{ lie in the same grain} \quad (8)$$

## Results and Discussion

Depolarized light scattering data from T50 and T900 are shown in Figure 1, where the intensity ( $I$ ) is plotted as a function of scattering vector,  $q$  ( $q = 4\pi \sin(\theta/2)/\lambda$ , where  $\theta$  is the scattering angle and  $\lambda = 633$  nm). For reference, we also show data obtained in the disordered state, prior to tempering. The scattering signal in the accessible  $q$ -range increases with increasing tempering time and eventually saturates. The data from T900 represent the saturated signal. The scattering profiles from both T50 and T900 were azimuthally symmetric. It is thus appropriate to interpret these data in terms of a correlation function that depends on  $r = |\mathbf{r} - \mathbf{r}'|$  alone. However, several different correlation functions can give indistinguishable intensity profiles; thus scattering alone cannot uniquely determine structure. We consider two forms for the correlation functions.<sup>8-12</sup>

If the correlation function is exponential

$$C(r) = \exp(-r/\kappa) \quad (9)$$

then eq 5 requires the intensity profile to be square Lorentzian:

$$I(q) = \frac{I_0}{(1 + q^2 \kappa^2)^2} \quad (10)$$

If the correlation function is Gaussian

$$C(r) = \exp(-r^2/\omega^2) \quad (11)$$

then eq 5 requires the intensity profile to be also Gaussian:<sup>13</sup>

$$I(q) = I_0 \exp[-q^2 \omega^2/4] \quad (12)$$

The solid curves in Figure 1 are least-squares square Lorentzian fits through the data, while the dashed curves represent least-squares Gaussian fits through the data.  $I_0$ ,  $\kappa$ , and  $\omega$  were treated as free parameters. It is evident that both forms of the correlation function

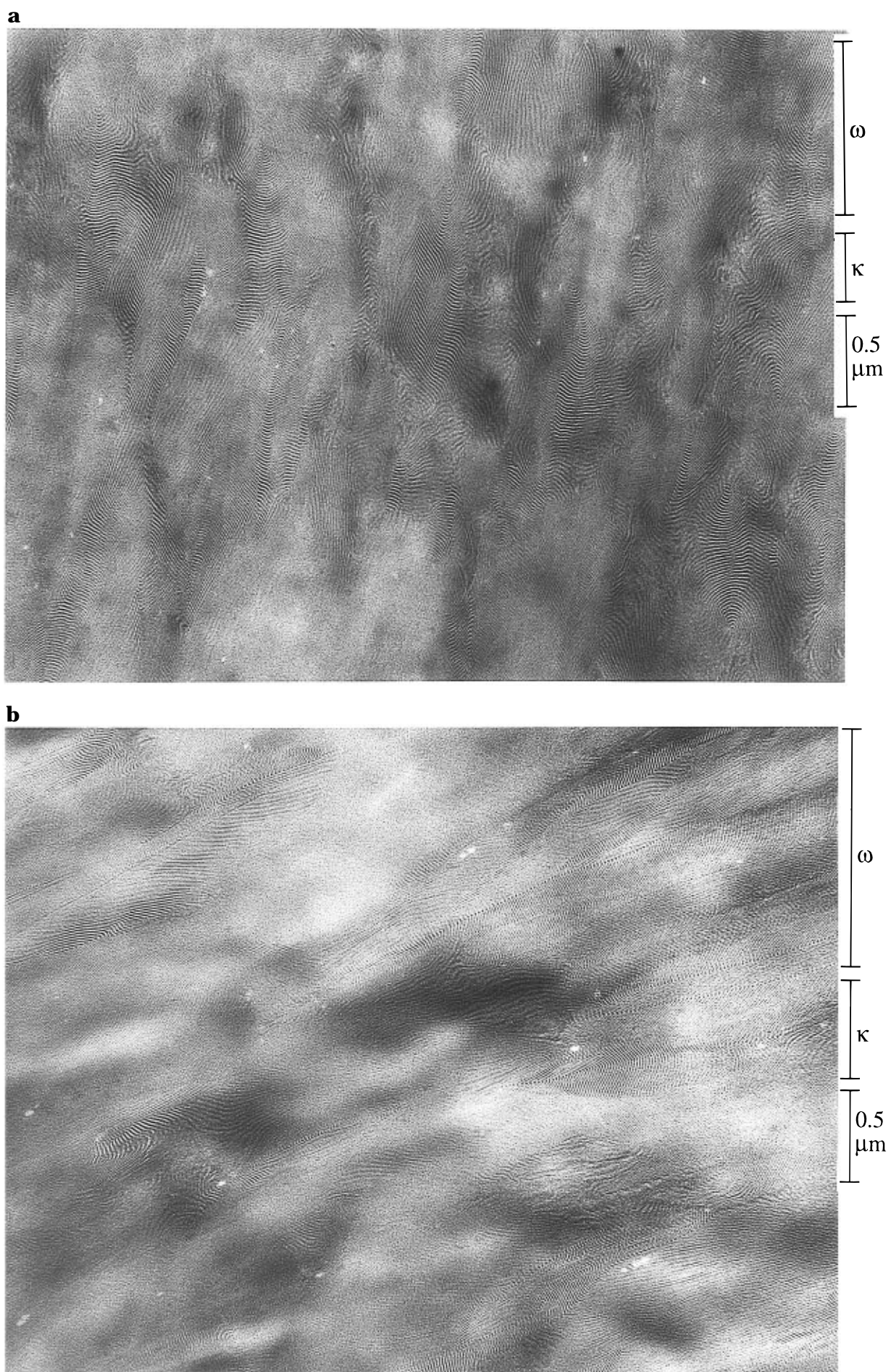


**Figure 2.** Typical transmission electron micrographs from samples (a) T50 and (b) T900. The correlation lengths obtained from depolarized light scattering measurements ( $\kappa$  and  $\omega$ ) are shown on the right-hand side of the micrographs.

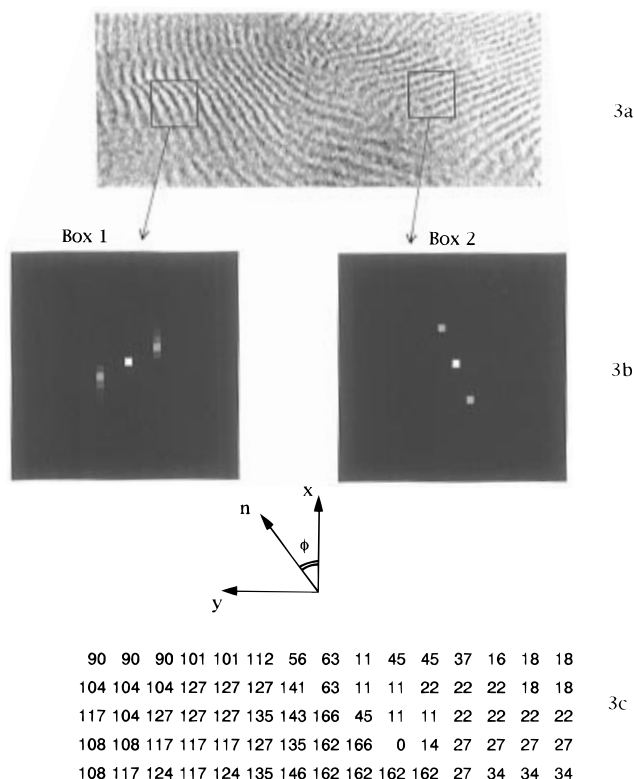


**Figure 3.** Procedure used to obtain the correlation function from transmission electron micrographs. (a) The image is digitized and divided into boxes. (b) The Fourier transform of the data within the boxes is computed. (c) A matrix of angles,  $\phi$ , is generated from the Fourier transform. For the sake of clarity, every other calculated angle is shown.

**Table 1. Correlation Lengths,  $\kappa$  and  $\omega$ , Obtained by Light Scattering**

sample	$\kappa$ ( $\mu\text{m}$ )	$\omega$ ( $\mu\text{m}$ )
T50	0.37	0.95
T900	0.54	1.30

are consistent with the scattering data. The limited  $q$ -range over which the light scattering data were collected is insufficient to distinguish between these different functional forms for  $C(r)$ . The correlation function parameters obtained from this fitting procedure are summarized in Table 1. Regardless of the assumed form of the correlation function, the correlation length of T50 is smaller than that of sample T900. This is consistent with observations of grain growth in other materials such as metals.<sup>14</sup>

In Figure 2 we show typical transmission electron micrographs from T50 (Figure 2a) and T900 (Figure 2b), respectively.  $\text{OsO}_4$  selectively stains the polyisoprene lamellae. In both micrographs one observes areas within which coherent order prevails. The bars on the right of the micrographs represent the correlation lengths ( $\kappa$  and  $\omega$ ) obtained from light scattering. Visual observation of the micrographs indicates that the correlation length in T50 is smaller than that in T900, which is in qualitative agreement with the light scattering results.

A quantitative comparison between light scattering and electron microscopy can be made by directly computing the correlation function from the TEM images. Negatives of the TEM images were digitized using an Epson 1200C digitizer. Lamellar orientations were computed by a *local two-dimensional Fourier analysis*. The methodology is illustrated in Figure 3. Each image was divided into overlapping  $64 \text{ nm} \times 64 \text{ nm}$  squares with centers separated by 20 nm, and the image within

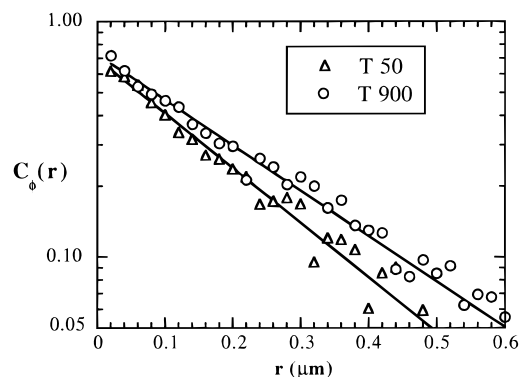


**Figure 4.** Plot of the correlation function,  $C(r)$ , after baseline subtraction, based on model 1, deduced from the transmission electron micrographs. The solid lines represent results of regression analysis. Baseline values of 0.092 for T50 and 0.075 for T900 were obtained from the regression analysis. The error bars due to counting statistics are smaller than the size of the symbols.

this square was stored as a  $32 \times 32$  element array of 8 bit integers (Figure 3a). The local Fourier transforms obtained from two typical squares are shown in Figure 3b. The peak at the origin (center of square) is the “dc” Fourier component and is related to the average intensity. The two symmetrical peaks at finite spatial frequencies are related to the periodic nature of the data and can be used to obtain local orientation and period.

The line through the peaks gives  $\phi$ , the angle between the projected local layer normal and the  $x$ -axis, defined in Figure 3. If the finite frequency peaks were found to lie in the four pixels adjacent to the dc peak, then it was assumed that the local periodic signal cannot be resolved. This may occur if the in-plane layer spacing exceeds the box size or if the local image quality is poor. Such points were skipped in the calculation of  $C(r)$ . The values of  $\phi$  obtained at each location,  $\mathbf{r}$ , on the micrograph in Figure 3a are given in Figure 3c. The values of  $\phi(\mathbf{r})$  toward the left side of the micrograph are in the vicinity of  $120^\circ$ , while those toward the right side of the micrograph are in the vicinity of  $20^\circ$ . This is in good agreement with expectations based on visual observation of Figure 3a.

The function  $C(r)$  was obtained using the two models described in the theory section:

**Model 1:** Random pairs of points,  $\mathbf{r}$  and  $\mathbf{r}'$ , were chosen on a digitized micrograph, and the local Fourier transform analysis gave  $\phi(\mathbf{r})$  and  $\phi(\mathbf{r}')$ . The ensemble averages,  $\langle \cos[2\{\phi(\mathbf{r}) - \phi(\mathbf{r}')\}] \rangle$ , for T50 and T900 were computed by repeating this procedure  $10^6$  times per micrograph; three independent micrographs were used for each sample. The distance scale,  $r = |\mathbf{r} - \mathbf{r}'|$ , was discretized into 20 nm interval bins. We found  $C(r) = \langle \cos[2\{\phi(\mathbf{r}) - \phi(\mathbf{r}')\}] \rangle$ —defined by eq 7—for T50 and T900 to be approximately exponential, with baselines of 0.18 and 0.23  $\mu\text{m}$  for samples T50 and T900, respectively. The baseline values, which were estimated by nonlinear regression, did not change when the number of points sampled per micrograph was increased. This indicates a small orientation bias in the micrographs. The bias may be due to the limited area used to obtain  $C(r)$  from TEM or due to a weak global anisotropy in the samples themselves, caused by uncontrolled processes that occurred during heat treatment and microtoming. The correlation functions, after baseline subtraction, are plotted in Figure 4. The correlation lengths,  $\kappa$ , obtained from these data were 0.18 and 0.23  $\mu\text{m}$  for samples T50 and T900, respectively.

**Model 2:** The correlation function was computed by choosing a random location,  $\mathbf{r}$ , on a digitized micrograph, computing  $\phi(\mathbf{r})$ , traveling along a random direction,<sup>15</sup>

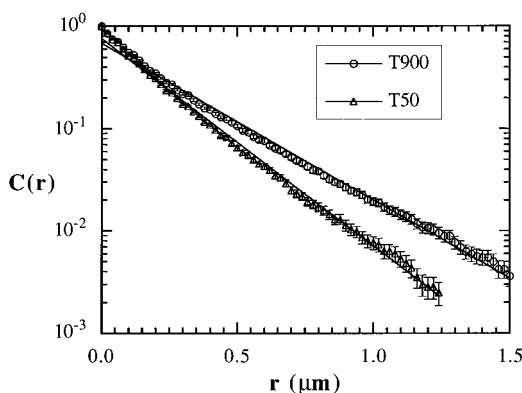


**Figure 5.** Plot of the correlation function based on model 2, deduced from the transmission electron micrographs ( $\Delta\phi = 30^\circ$ ). The solid lines represent results of regression analysis. The error bars are based on counting statistics.

**Table 2. Correlation Length,  $\kappa$ , Obtained by Electron Microscopy**

sample	$\kappa$ ( $\mu\text{m}$ ) using model 1	$\kappa$ ( $\mu\text{m}$ ) using model 2	
		$\Delta\theta = 30^\circ$	$\Delta\theta = 15^\circ$
T50	0.19	0.21	0.13
T900	0.23	0.28	0.19

and examining  $\phi(\mathbf{r}')$ . The discretization of  $r = |\mathbf{r} - \mathbf{r}'|$  and the images used here were the same as those used to compute  $C(r)$  from model 1. If  $|\phi(\mathbf{r}) - \phi(\mathbf{r}')|$  was less than a prescribed tolerance,  $\Delta\phi$ , then  $\mathbf{r}$  and  $\mathbf{r}'$  were considered to lie within the same grain and "one" was input in the corresponding bin. The distance  $r$  was gradually increased until a location  $\mathbf{r}^*$  was reached such that  $|\phi(\mathbf{r}') - \phi(\mathbf{r}^*)|$  was greater than  $\Delta\phi$ . "Zeros" were input into all bins with  $r \geq |\mathbf{r} - \mathbf{r}^*|$ . This procedure was repeated 4000 times for different  $\mathbf{r}'$  locations on each micrograph. The fraction of "ones" in each bin gives the correlation function at the corresponding  $r$ , as defined in eq 8. Since correlations beyond  $\mathbf{r}^*$  are ignored in this model, the computed correlation function must asymptotically go to zero for large  $r$ ; baseline subtraction was not needed.

The correlation functions for  $\Delta\phi = 30^\circ$  are shown in Figure 5. These correlation functions are approximately exponential with correlation lengths,  $\kappa$ , of 0.21 and 0.28  $\mu\text{m}$  for samples T50 and T900, respectively. Model calculations of scattering profiles indicate that  $\Delta\phi$  should be less than or equal to  $30^\circ$ .<sup>16</sup> The correlation lengths depend on the prescribed tolerance,  $\Delta\phi$ ; more stringent definitions led to smaller correlation lengths. Nevertheless, the functional form of  $C(r)$  and the relative changes with tempering history are independent of the choice of  $\Delta\phi$ . For instance,  $\kappa$  values obtained for  $\Delta\phi = 15^\circ$  were 0.13 and 0.19 for samples T50 and T900, respectively. The ratio  $\kappa(\text{T900})/\kappa(\text{T50})$  is 1.33 for  $\Delta\phi = 30^\circ$  and 1.41 for  $\Delta\phi = 15^\circ$ . These ratios are in reasonable agreement with the model 1 result of 1.28 and the light scattering result of 1.48.

We are not aware of any other study in which orientation correlations in quiescently quenched block copolymers have been examined in both position space ( $r$ ) and reciprocal space ( $q$ ). The correlation lengths obtained in position space by TEM are summarized in Table 2. They are within a factor of 2 of the values obtained in reciprocal space by light scattering (see Table 1). However, regardless of the computation scheme, the values of  $\kappa$  obtained by TEM are consistently smaller than those obtained by light scattering. Further work is required to understand the origin of this discrepancy.

## Concluding Remarks

We have studied the nature of orientation correlations in quiescently quenched block copolymer lamellae by light scattering and electron microscopy. Both kinds of experiments were necessary to provide a complete picture. The strength of light scattering is that it samples, simply and nondestructively, the statistical properties of a large number of grains (about 1 billion in this case). This is in contrast to electron microscopy where global averaging is unfeasible. The total area examined in this work by TEM averages to about 50 grains per sample. On the other hand, electron microscopy gives the position-space structure directly and has revealed the exponential nature of the correlation function, whereas the functional form was not uniquely determined by light scattering. Both techniques are in agreement in showing that correlation lengths increase with longer tempering times. Whether these features are common to all quiescently quenched lamellar materials or specific to the particular block copolymer sample studied here remains to be established.

**Acknowledgment.** Financial support from the National Science Foundation to Polytechnic University (Grants CTS-9308164, DMR-9307098, and DMR-945-7950) and the 3M Non-tenured Faculty Award to N.P.B. is gratefully acknowledged. We thank Said Nourbakhsh, Yao Wang, and Sung Whang for helpful discussions.

## References and Notes

- (1) de Gennes, P.-G.; Prost, J. *The Physics of Liquid Crystals*, 2nd ed.; Oxford: New York, 1993.
- (2) Chandrasekar, S. *Liquid Crystals*, 2nd ed.; Cambridge: New York, 1992.
- (3) Demus, D.; Richter, L. *Textures of Liquid Crystals*; Verlag Chemie: New York, 1978.
- (4) Gido, S. P.; Thomas, E. L. *Macromolecules* **1994**, *27*, 6137 and references therein.
- (5) Levitz, P.; Ehret, G.; Sinha, S. K.; Drake, J. M. *J. Chem. Phys.* **1994**, *95*, 6151.
- (6) Murray, C. A. In *Bond-Orientational Order in Condensed Matter Systems*; Strandburg, K. J., Ed.; Springer-Verlag: New York, 1992; p 317 and references therein.
- (7) Lin, C. C.; Jonnalagadda, S. V.; Kesani, P. K.; Dai, H. J.; Balsara, N. P. *Macromolecules* **1994**, *27*, 7769.
- (8) (a) Balsara, N. P.; Garetz, B. A.; Dai, H. J. *Macromolecules* **1992**, *25*, 6072. (b) Garetz, B. A.; Newstein, M. C.; Dai, H. J.; Jonnalagadda, S. V.; Balsara, N. P. *Macromolecules* **1993**, *26*, 3151.
- (9) Stein, R. S.; Wilson, P. R. *J. Appl. Phys.* **1962**, *33*, 1914.
- (10) Milner, S. T. *Macromolecules* **1993**, *26*, 2974.
- (11) Flygare, W. H. *Molecular Structure and Dynamics*; Prentice-Hall: Englewood Cliffs, NJ, 1978.
- (12) Debye, P.; Beuche, A. M. *J. Appl. Phys.* **1949**, *20*, 518.
- (13) We correct an error in eq 19 of ref 8b; the right-hand side of that equation should be multiplied by a factor of (1/2).
- (14) Van Vlack, L. H. *Elements of Materials Science*, 5th ed.; Addison-Wesley: Reading, MA, 1987.
- (15) A random number generator was used to choose one of eight directions:  $\pm\hat{x}$ ,  $\pm\hat{y}$ , and  $\pm(\hat{x}\pm\hat{y})$ .
- (16) To study the effect of continuous variation of lamellar orientation, depolarized light scattering profiles from "pairs" of lamellar grains with a fixed angle between the optic axes ( $\Psi$ ) were computed following the treatment given in ref 17. When  $\Psi \leq 20^\circ$ , the calculated scattering patterns were nearly indistinguishable from that obtained from a single grain ( $\Psi = 0$ ); the maximum deviation was at  $q = 0$ , and it was less than 10%. When  $\Psi = 30^\circ$ , the maximum deviation was 20%. We thus conclude that light scattering is sensitive to changes in lamellar orientation that are in the vicinity of  $30^\circ$ , or larger.
- (17) Newstein, M. C.; Garetz, B. A.; Dai, H. J.; Balsara, N. P. *Macromolecules* **1995**, *28*, 4587.